

Measurement of the Decay $\Upsilon(2S) \rightarrow \pi\pi \Upsilon(1S)^*$

D. Gelpman,^(lt) B. Lurz,^(f) D. Antreasyan,⁽ⁱ⁾ D. Aschman,^(b) D. Besset,^(k)
 J. K. Bienlein,^(e) E. D. Bloom,^(l) I. Brock,^(c) R. Cabenda,^(k) A. Cartacci,^(g) M. Cavalli-Sforza,^(k)
 R. Clare,^(l) G. Conforto,^(g) S. Cooper,^(l) R. Cowan,^(k) D. Coyne,^(k) C. Edwards,^(a)
 A. Engler,^(c) G. Folger,^(f) A. Fridman,^(ht) J. Gaiser,^(l) G. Godfrey,^(l) F. H. Heimlich,^(h)
 R. Hofstadter,^(l) J. Irion,⁽ⁱ⁾ Z. Jakubowski,^(d) S. Keh,^(m) H. Kilian,^(m) I. Kirkbride,^(l) T. Kloiber,^(e)
 W. Koch,^(e) A. C. König,^(j) K. Königsmann,^(m) R. W. Kraemer,^(c) R. Lee,^(lt) S. Leffler,^(l)
 R. Lekebusch,^(h) P. Lezoch,^(h) A. M. Litke,^(lt) W. Lockman,^(l) S. Lowe,^(l) D. Marlow,^(c)
 W. Maschmann,^(h) T. Matsui,^(l) F. Messing,^(c) W. J. Metzger,^(j) B. Monteleoni,^(g) R. Nernst,^(h)
 C. Newman-Holmes,^(k) B. Niczyporuk,^(th) G. Nowak,^(d) C. Peck,^(a) P. G. Pelfer,^(g) B. Pollock,^(l)
 F.C. Porter,^(a) D. Prindle,^(c) P. Ratoff,^(a) B. Renger,^(c) C. Rippich,^(c) M. Scheer,^(m)
 P. Schmitt,^(m) M. Schmitz,^(e) J. Schotanus,^(j) A. Schwarz,^(l) D. Sievers,^(h) T. Skwarnicki,^(e#)
 K. Strauch,⁽ⁱ⁾ U. Strohbush,^(h) J. Tompkins,^(l) H. J. Trost,^(e) R. T. Van de Walle,^(j) H. Vogel,^(c)
 U. Volland,^(f) K. Wacker,^(l) W. Walk,^(j) H. Wegener,^(f) D. Williams,⁽ⁱ⁾ P. Zschorsch,^(e)

(THE CRYSTAL BALL COLLABORATION)

- (a) *California Institute of Technology, Pasadena, USA*
- (b) *University of Cape Town, South Africa*
- (c) *Carnegie-Mellon University, Pittsburgh, USA*
- (d) *Cracow Institute of Nuclear Physics, Cracow, Poland*
- (e) *Deutsches Elektronen Synchrotron DESY, Hamburg, Germany*
- (f) *Universität Erlangen-Nürnberg, Erlangen, Germany*
- (g) *INFN and University of Firenze, Italy*
- (h) *Universität Hamburg, I. Institut für Experimentalphysik, Hamburg, Germany*
- (i) *Harvard University, Cambridge, USA*
- (j) *University of Nijmegen and NIKHEF-Nijmegen, The Netherlands*
- (k) *Princeton University, Princeton, USA*
- (l) *Department of Physics, HEPL, and Stanford Linear Accelerator Center
Stanford University, Stanford, USA*
- (m) *Universität Würzburg, Würzburg, Germany*

Submitted to *Physical Review D*

* This work was supported in part by the U.S. Department of Energy under Contract No. DE-AC03-76SF00515.

ABSTRACT

We have investigated the hadronic transitions $\Upsilon(2S) \rightarrow \pi^0\pi^0$ $\Upsilon(1S) \rightarrow \gamma\gamma\gamma l^+l^-$ ($l = \mu$ or e) and $\Upsilon(2S) \rightarrow \pi^+\pi^-$ $\Upsilon(1S) \rightarrow \pi^+\pi^-e^+e^-$ using the Crystal Ball detector at the DORIS II e^+e^- storage ring. Using the present world average value of $B_{\mu}(\Upsilon(1S)) = (2.9 \pm 0.3)\%$ we derive branching ratios $B(\Upsilon(2S) \rightarrow \pi^0\pi^0 \Upsilon(1S)) = (8.0 \pm 1.5)\%$ and $B(\Upsilon(2S) \rightarrow \pi^+\pi^- \Upsilon(1S)) = (16.9 \pm 4.0)\%$. We also present results on the invariant mass spectra and the angular distributions of the di-pion system.

Introduction

Hadronic transitions between heavy quark-antiquark bound states have been studied both experimentally and theoretically. The decay $\Upsilon(2S) \rightarrow \pi^+\pi^-\Upsilon(1S)$ was the first observed hadronic transition in the $b\bar{b}$ system^{1,2,3}. Whereas this transition has since been studied^{4,5} with high statistics, only one measurement⁶ of the transition $\Upsilon(2S) \rightarrow \pi^0\pi^0\Upsilon(1S)$ has been performed up to now. A comparison of the charged and the neutral $\pi\pi$ transitions is a test of the isospin invariance of this process.

Theory describes the hadronic decay $\Upsilon(2S) \rightarrow \pi\pi\Upsilon(1S)$ and $\psi' \rightarrow \pi\pi J/\psi$ as a two step process. First the excited quarkonium state radiates gluons. Since the available energy for the gluons is small, the emission process cannot be treated in perturbation theory. However, Gottfried⁷ and Yan⁸ have shown that a multipole expansion of the gluonic field converges rapidly since the dimensions of the radiating heavy quark system are small compared to the wavelength of the emitted gluons. In a second step the gluons fragment into light hadrons; here the properties of the di-pion system are determined by using partial conservation of axial-vector current (PCAC) and current algebra^{8,9}. This picture, together with the observed^{5,6,10} isotropic angular distributions for the decay of this system, leads to the prediction of an invariant $\pi\pi$ mass distribution which is peaked towards high values. This prediction has been verified for the transition $\Upsilon(2S) \rightarrow \pi^+\pi^-\Upsilon(1S)$ ^{4,5,6} and $\psi' \rightarrow \pi\pi J/\psi$ ^{10,11}; however, for the $\pi^+\pi^-$ transition from $\Upsilon(3S)$ to $\Upsilon(1S)$ an invariant $\pi\pi$ mass distribution has been observed^{12,13} which is inconsistent with the expectation from theory. Thus hadronic transitions between heavy quark-antiquark bound states still deserve a careful study.

With the Crystal Ball detector at DORIS II we have studied the hadronic transitions $\Upsilon(2S) \rightarrow \pi^0\pi^0\Upsilon(1S)$ (where the final state $\Upsilon(1S)$ decays into a lepton pair e^+e^- or $\mu^+\mu^-$) and $\Upsilon(2S) \rightarrow \pi^+\pi^-\Upsilon(1S) \rightarrow \pi^+\pi^-e^+e^-$. We present measurements of the branching ratios and results on the invariant

mass spectra and the angular distributions of the di-pion system.

Detector and Trigger

The Crystal Ball detector is a nonmagnetic calorimeter especially designed for measuring electromagnetically showering particles. The major component of the detector is a highly segmented spherical array of 672 NaI(Tl) crystals covering 93% of the total solid angle. Each crystal is 16 radiation lengths long. The geometry of the array is based on an icosahedron. Each of the twenty triangular faces, referred to as "major triangles", is subdivided into four "minor triangles" each consisting of nine individual crystals. The solid angle coverage of the Ball is extended to 98% of 4π steradians by NaI(Tl) endcaps. The energy resolution of

$$\frac{\sigma(E)}{E} = \frac{2.6\%}{E^{\frac{1}{4}}} \quad (\text{E in GeV})$$

for electromagnetically showering particles makes the Ball well suited for measuring energies of photons and electrons. The most probable energy deposited by minimum ionizing particles is about 210 MeV. The high segmentation of the detector provides a measurement of the direction of photons and electrons with an angular resolution of 1-2 degrees, slightly dependent on energy. Tracking of charged particles is performed by three double layers of proportional tube chambers with charge division readout, resulting in an angular resolution for charged tracks of about 1 degree. The direction of non-interacting charged particles can also be determined from their energy deposition in the crystals with an angular resolution of 2 degrees. The luminosity is determined by measuring large angle Bhabha scattering; a check is made by also measuring Bhabha scattering at small angles.

The analysis of the decay $\Upsilon(2S) \rightarrow \pi\pi\Upsilon(1S)$ is based on a data sample of 193 000 $\Upsilon(2S)$ decays corresponding to an integrated luminosity of

60.6 pb^{-1} . The search for events containing approximately back-to-back electron or muon pairs plus additional energy clusters in the central calorimeter is performed by requiring at least one of the following hardware triggers:

a) A total energy trigger, which requires an energy sum in the Ball of more than 1.7 GeV. For $\pi\pi e^+e^-$ events completely contained in the fiducial volume of the detector, this trigger is 100% efficient.

b) A topology trigger, which is based on the fact that the Ball can be divided ten different ways into approximate hemispheres. This trigger requires that, for each division, both hemispheres contain at least one major triangle with more than 150 MeV and that the total energy deposition in the Ball exceeds 770 MeV.

c) A trigger, which requires two approximately back-to-back minor triangles each containing more than 85 MeV and a total energy of more than 220 MeV in the Ball.

Triggers b) and c) are designed to accept events with at least two almost back-to-back particles and a low total energy deposition. From a measurement of the trigger thresholds and a Monte Carlo simulation of the triggers, we estimate the overall trigger efficiency to be greater than 98% for $\pi^0\pi^0\mu^+\mu^-$ events fully contained in the fiducial volume of the detector.

The Decay $\Upsilon(2S) \rightarrow \pi^0\pi^0\Upsilon(1S)$

For events of the type $\pi^0\pi^0l^+l^-$ ($l = \mu$ or e) we require exactly 6 particles in the Ball within $|\cos \Theta| \leq 0.85$, where Θ is the angle between any particle and the incoming positron beam direction. To avoid systematic effects due to varying chamber performance we do not use the chamber information for charged particle tagging or angle measurements in the $\pi^0\pi^0l^+l^-$ channel. All particle directions for this channel are therefore based on the energy deposition in the Ball with the assumption that the particles originate from $z=0$. The lepton pair is identified by finding two particles with an acollinearity

smaller than 17 degrees¹⁴. Furthermore, for electron pair candidates each of the two particles is required to have an energy deposition of more than 3.5 GeV whereas for each muon candidate an observed energy between 150 MeV and 330 MeV is required with essentially all of the energy contained in only 1 or 2 crystals. The selection criteria for muon candidates are based on studies of $e^+e^- \rightarrow \mu^+\mu^-$ annihilation events. The lateral energy distribution of the other four particles, the photon candidates, must be consistent with that of electromagnetically showering particles, and the energy deposition of each particle has to be greater than 10 MeV. In addition, the sum of the energy deposited by the photon candidates is required to be greater than 160 MeV. To ensure a clean energy measurement of the photons we require the opening angle between any two particles to be larger than 26° ($\cos \theta_{i,j} < 0.9$). For events of the type $\gamma\gamma\gamma\mu^+\mu^-$ we apply additional cuts on event cleanliness: the energy measured by the endcaps must not exceed 40 MeV, and the energy measured in the Ball which is not assigned to any of the six particles must be less than 80 MeV.

All events surviving these cuts are kinematically fit to the hypothesis $e^+e^- \rightarrow \Upsilon(2S) \rightarrow \gamma\gamma\gamma l^+l^-$ using energy and momentum conservation. This results in a two constraint (2-C) fit since the measured energies of the leptons are not used¹⁵. For events passing the fit with a confidence level larger than 5%, we plot in Fig. 1 the two photon invariant mass $m_{\gamma\gamma}$ of each pairing combination versus the invariant mass of the remaining photons. The scatter plot contains three entries per event and shows a clear clustering in the mass region of two π^0 s. The bulk of the background in Figure 1 appears in the region of low $\gamma\gamma$ mass combinations and is due to radiative QED events with additional spurious energy in the detector. An additional contribution to the background originates from good $\pi^0\pi^0 l^+l^-$ events where one photon escapes detection and is mimicked by spurious energy in the detector. The box indicates our cut at ± 22 MeV on both axes around the π^0 mass. This cut corresponds to approximately ± 3 standard deviations of our π^0 mass

resolution. In Fig. 2 we plot the mass difference $\Delta M = M(\Upsilon(2S)) - M_{recoil}$ for events with at least one combination of the four photons with masses $m_{\gamma\gamma}$ within the above limits. M_{recoil} is the mass recoiling against the four photon system and is calculated from the four-momentum vectors of the photons. The FWHM of 45 MeV is in good agreement with the Monte Carlo expectation based on the energy and angular resolution of the photons as indicated by the solid curve in Fig. 2. We note that our measured π^0 mass distribution as well as the mass difference $M(\Upsilon(2S)) - M(\Upsilon(1S))$ obtained from the four measured photon energies is systematically shifted to lower values on the order of 5%. We have corrected the photon energies so that the measured π^0 mass distribution and the mass difference peak at their expected values¹⁶.

Our final data sample contains 44 events of the type $\gamma\gamma\gamma\gamma\mu^+\mu^-$ and 46 events of the type $\gamma\gamma\gamma\gamma e^+e^-$ with a mass difference ΔM between 503 MeV and 623 MeV. The background is estimated by averaging over equal area sidebands on each side of the signal region. We estimate one background event in the $\gamma\gamma\gamma\gamma\mu^+\mu^-$ sample and two events in the $\gamma\gamma\gamma\gamma e^+e^-$ sample which we subtract from the final number of events for the branching ratio calculations.

Possible sources of background in our data sample are the processes $\Upsilon(2S) \rightarrow \pi^0\pi^0 \Upsilon(1S)$ with the $\Upsilon(1S)$ decaying into $\tau^+\tau^-$, radiative QED events with additional spurious energy in the detector, cosmic ray events, and low multiplicity hadronic events originating from $\Upsilon(2S)$ decays or continuum processes. The τ pair contribution is studied by Monte Carlo simulation and the background is estimated to be less than one event in the muon channel and negligible in the electron channel. We estimate the cosmic ray background to be negligible based on the timing of the energy signals in the NaI(Tl) modules relative to the time of the beam crossing in the signal events. To estimate the background from QED processes and hadronic decays we have analyzed approximately $30 pb^{-1}$ of $\Upsilon(1S)$ data. This corresponds to

about half the number of the continuum events and to about 1.5 times the number of resonance decays in our analyzed $\Upsilon(2S)$ data sample. We find one $\gamma\gamma\gamma\mu^+\mu^-$ event within the mass difference window 503 MeV to 623 MeV. These studies are consistent with the above sideband estimate of three background events.

The acceptance for the decay $\Upsilon(2S) \rightarrow \pi^0\pi^0 \Upsilon(1S) \rightarrow \gamma\gamma\gamma\gamma l^+l^-$ is evaluated using a model where the $\pi^0\pi^0$ system is emitted in an S-wave and has spin zero. Our model includes the measured 70% beam polarization of DORIS II at the energy of the $\Upsilon(2S)$ resonance; this affects the angular distribution of the leptonic decays of the $\Upsilon(1S)$. The calculated acceptance depends only weakly on the degree of polarization. The Monte Carlo simulation for electrons and photons is done with the EGS code¹⁷. Muons are simulated by adding the energy distribution from observed muons in $e^+e^- \rightarrow \mu^+\mu^-$ events to the Monte Carlo events. To include the effects of beam related background on the detection efficiency, the energy observed in random beam crossing triggers is added to each Monte Carlo event.

In order to obtain the detection efficiency independent of assumptions about the shape of the di-pion mass distribution, we determine the acceptance as a function of the invariant di-pion mass $M_{\pi^0\pi^0}$. The curve in Fig. 3 is the summed acceptance of the $\pi^0\pi^0 e^+e^-$ and $\pi^0\pi^0 \mu^+\mu^-$ decay modes. The acceptance shows a large variation over the kinematic range of $M_{\pi^0\pi^0}$ due to increasing (decreasing) overlap probability between photons from different pions as $M_{\pi^0\pi^0}$ approaches the lower (higher) kinematic limit. The acceptance corrected number of events is obtained by binning the data in $M_{\pi^0\pi^0}$ and correcting each bin by the efficiency averaged over that bin. From the number of observed and efficiency corrected events of both decay modes we obtain average efficiencies of $\epsilon_{ee\pi^0\pi^0} = 0.10 \pm 0.01$ and $\epsilon_{\mu\mu\pi^0\pi^0} = 0.09 \pm 0.01$, where the errors are almost entirely systematic. The main contributions to the systematic errors are the uncertainties in modelling the detector, the simulation of the background energy in the Ball,

and the sensitivity of the branching ratios to variations of the cuts. The overall systematic error is obtained by adding the different contributions in quadrature.

From the final event sample we obtain the invariant $\pi^0\pi^0$ mass distribution shown as the histogram in Fig. 4. Clearly, a mass distribution according to phase space (dashed curve) is excluded by the data. We fit the observed mass spectrum to three different theoretical expressions^{8,18,19} folded with our experimental resolution in $M_{\pi^0\pi^0}$ of 8 MeV and the acceptance curve of Fig. 3. All three theoretical expressions contain a term $(M_{\pi\pi}^2 - \text{constant})^2$ which accounts for the peaking of the di-pion mass distribution at high values. Within the drawing accuracy, the fits to all three theoretical models are represented by the solid curve in Fig. 4. The functional form and the value of the fitted parameter of each model are listed in Table 1. These values have been determined previously^{4,5,6} only for the decay $\Upsilon(2S) \rightarrow \pi^+\pi^-\Upsilon(1S)$. Our results are consistent with those measurements. A previous measurement⁶ of $\Upsilon(2S) \rightarrow \pi^0\pi^0\Upsilon(1S)$ also shows a peaked di-pion mass distribution, in qualitative agreement with our data.

We also extract from our data the angular distributions for $\cos\theta_{\pi^0\pi^0}$ and $\cos\theta_{\pi^0}^*$. The angle $\theta_{\pi^0\pi^0}$ is the polar angle of the di-pion momentum vector with respect to the beam axis in the laboratory frame. The angle $\theta_{\pi^0}^*$ is the polar angle of the π^0 direction in the rest frame of the $\pi\pi$ system, where the z-axis is parallel to the beam axis. This angle is sensitive to the spin of the $\pi\pi$ system²⁰. Figs. 5(a),(b) show the observed distributions superimposed with the Monte Carlo prediction (solid curve), which is calculated using the measured $M_{\pi^0\pi^0}$ mass distribution and isotropic decay distributions as expected for a di-pion system of spin zero emitted in an S-wave. The data for $\cos\theta_{\pi^0}^*$ are in good agreement with isotropy. For the distribution in $\cos\theta_{\pi^0\pi^0}$ the confidence level of the agreement between the data and the prediction from isotropy is only 3%. This low confidence level is due to the high number of counts at $\cos\theta_{\pi^0\pi^0} = -0.5$. We have looked for and have

found no systematic effects which can explain this. We believe that this high bin is due to a statistical fluctuation and that this distribution is consistent with isotropy.

From the number of background corrected events, the detection efficiencies, and the number of $(193 \pm 15) \times 10^3$ produced $\Upsilon(2S)$ decays we obtain the following product branching ratios (the first error being statistical, the second systematic):

$$B(\Upsilon(2S) \rightarrow \pi^0 \pi^0 \Upsilon(1S)) \times B(\Upsilon(1S) \rightarrow e^+ e^-) = (2.2 \pm 0.4 \pm 0.2) \times 10^{-3},$$

$$B(\Upsilon(2S) \rightarrow \pi^0 \pi^0 \Upsilon(1S)) \times B(\Upsilon(1S) \rightarrow \mu^+ \mu^-) = (2.4 \pm 0.4 \pm 0.3) \times 10^{-3}.$$

The error on the number of produced $\Upsilon(2S)$ decays is mainly systematic and mostly due to the uncertainty in our hadronic detection efficiency. Assuming lepton universality, we average the electron and muon results and find a product branching ratio of

$$B(\Upsilon(2S) \rightarrow \pi^0 \pi^0 \Upsilon(1S)) \times B(\Upsilon(1S) \rightarrow l^+ l^-) = (2.3 \pm 0.3 \pm 0.3) \times 10^{-3}.$$

Dividing out the present world average value²¹ of the leptonic branching ratio $B_{\ell}(\Upsilon(1S)) = (2.9 \pm 0.3)\%$ we obtain $B(\Upsilon(2S) \rightarrow \pi^0 \pi^0 \Upsilon(1S)) = (8.0 \pm 1.5)\%$, where we have added the statistical and systematic errors in quadrature.

Our result is consistent with the recently published CUSB⁶ value of $B(\Upsilon(2S) \rightarrow \pi^0 \pi^0 \Upsilon(1S)) = (10.3 \pm 2.3)\%$. The present average value of the branching ratio $B(\Upsilon(2S) \rightarrow \pi^+ \pi^- \Upsilon(1S))$, derived from exclusive and inclusive measurements²², is $(18.8 \pm 1.0)\%$. Using this value and our measurement for the $\pi^0 \pi^0$ channel we obtain a ratio $\frac{\Gamma(\Upsilon(2S) \rightarrow \pi^0 \pi^0 \Upsilon(1S))}{\Gamma(\Upsilon(2S) \rightarrow \pi^+ \pi^- \Upsilon(1S))} = 0.43 \pm 0.07$. Taking into account phase space we expect this ratio to be 0.53 for an $I = 0$ isospin assignment of the $\pi\pi$ system, which is required if isospin is conserved. Our result agrees with this expectation with a confidence level of 11%.

The Decay $\Upsilon(2S) \rightarrow \pi^+\pi^-\Upsilon(1S)$

We also have studied the reaction $\Upsilon(2S) \rightarrow \pi^+\pi^-\Upsilon(1S)$. Here the $\Upsilon(1S)$ is required to decay into an e^+e^- pair in order to suppress hadronic background. As the event selection and data analysis for this channel are in many respects similar to the $\pi^0\pi^0e^+e^-$ decay, we stress only those cuts which differ from the previous analysis. We require two almost back-to-back particles with an energy of at least 3.5 GeV each, in addition to two particles depositing at least 50 MeV each. We require the two low energy particles, the pion candidates, to be charged. The charge requirement is necessary to reduce the background in this channel; however, the use of the tracking chambers in this analysis increases the overall systematic error. The energy deposited by both charged particles together has to exceed 160 MeV. This energy sum requirement for the two pion candidates is very efficient since the pions originating from the decay $\Upsilon(2S) \rightarrow \pi^+\pi^-\Upsilon(1S)$ are slow and will often stop in the Ball leaving at least their kinetic energy of about 280 MeV. To ensure clean energy measurements we require in addition:

- a) the opening angle between any two tracks to be larger than 32° ($\cos \theta_{i,j} < 0.85$),
- b) all four tracks to be well within the main calorimeter: $|\cos \Theta| \leq 0.85$,
- c) no additional particle with energy larger than 30 MeV in this solid angle, and
- d) less than 100 MeV of energy deposited in the endcap crystals.

Events surviving these selection criteria are subjected to a 3-C kinematic fit using the measured electron energies and constraining the e^+e^- mass to the $\Upsilon(1S)$ mass. After a cut on the confidence level of 10% we obtain a final sample of 169 events of the type $\Upsilon(2S) \rightarrow \pi^+\pi^-\Upsilon(1S) \rightarrow \pi^+\pi^-e^+e^-$.

— Possible sources of background to this reaction are the processes $\Upsilon(2S) \rightarrow \pi^+\pi^-\Upsilon(1S) \rightarrow \pi^+\pi^-\tau^+\tau^-$, the cascade decays $\Upsilon(2S) \rightarrow \gamma\gamma\Upsilon(1S)$, $\Upsilon(2S) \rightarrow \pi^0\pi^0\Upsilon(1S)$ and radiative QED events with photons misidentified

as charged particles. The first three background processes are evaluated with Monte Carlo techniques and are found to be negligible. The background due to radiative QED events with additional spurious energy in the detector is estimated by carrying out the above analysis on approximately 30 pb^{-1} of $\Upsilon(1S)$ data. We find 4 events satisfying all cuts. Based on twice the luminosity for our $\Upsilon(2S)$ data, we estimate a total of 8 background events to be subtracted from the final sample of 169 events for the calculation of the branching ratio.

The Monte Carlo model used to determine the overall detection efficiency incorporates the $M_{\pi\pi}$ mass distribution as given by Voloshin and Zakharov¹⁸ with the only parameter fixed at $\lambda = 2$. This choice is not crucial since our efficiency is almost constant over the whole $M_{\pi^+\pi^-}$ mass region. We obtain $\epsilon_{ee\pi^+\pi^-} = 0.17 \pm 0.03$, where the error is dominated by the systematics in the determination of the tube chamber tracking efficiency. This efficiency has been obtained by studying $e^+e^- \rightarrow \mu^+\mu^-$ events and is found to be $0.90^{+0.10}_{-0.12}$ per track.

From the final data sample we extract the invariant $M_{\pi^+\pi^-}$ mass distribution shown in Fig. 6. This spectrum exhibits the same behavior as that observed in our $\pi^0\pi^0$ analysis and that seen by other experiments²⁻⁶. We fit the observed mass spectrum to the three theoretical expressions^{8,18,19} corrected for acceptance and folded with our experimental resolution in $M_{\pi^+\pi^-}$ of 15 MeV. Within the drawing accuracy, all fits are again represented by one solid curve. The results from these fits, included in Table 1, are consistent with those found in the $\pi^0\pi^0$ analysis and those obtained by other experiments⁴⁻⁶.

We also obtain angular distributions for $\cos\theta_{\pi^+\pi^-}$ and $\cos\theta_{\pi^\pm}^*$. The definitions of these angles are identical to the ones for the neutral mode. Figs. 7(a),(b) show the data superimposed with the expectation from the Monte Carlo model as described above. Both angular distributions show

good agreement with the hypothesis of an isotropic emission of a spin zero di-pion system.

From the background corrected number of events, the detection efficiency, and $(193 \pm 15) \times 10^3 \Upsilon(2S)$ events we obtain the following branching ratio:

$$B(\Upsilon(2S) \rightarrow \pi^+\pi^- \Upsilon(1S)) \times B(\Upsilon(1S) \rightarrow e^+e^-) = (4.9 \pm 0.4 \pm 1.0) \times 10^{-3}.$$

With the average leptonic branching ratio²¹ $B_{\ell\ell}(\Upsilon(1S)) = (2.9 \pm 0.3)\%$ we obtain $B(\Upsilon(2S) \rightarrow \pi^+\pi^- \Upsilon(1S)) = (16.9 \pm 4.0)\%$, where the statistical and systematic errors are added in quadrature. This result is consistent with the present average value²² of $B(\Upsilon(2S) \rightarrow \pi^+\pi^- \Upsilon(1S)) = (18.8 \pm 1.0)\%$ derived from exclusive and inclusive measurements. For completeness, we present the ratio of our measured branching ratios for the neutral and charged pion transitions. In this ratio the common systematic uncertainty in the number of produced $\Upsilon(2S)$ resonance decays cancels. We find $\frac{\Gamma(\Upsilon(2S) \rightarrow \pi^0\pi^0 \Upsilon(1S))}{\Gamma(\Upsilon(2S) \rightarrow \pi^+\pi^- \Upsilon(1S))} = 0.47 \pm 0.11$, again consistent with an $I = 0$ assignment for the $\pi\pi$ system. Additionally we include our measurements for these channels with the previous world average values and obtain $\frac{\Gamma(\Upsilon(2S) \rightarrow \pi^0\pi^0 \Upsilon(1S))_{average}}{\Gamma(\Upsilon(2S) \rightarrow \pi^+\pi^- \Upsilon(1S))_{average}} = 0.46 \pm 0.06$.

Summary

We conclude that for the decay $\Upsilon(2S) \rightarrow \pi^0\pi^0 \Upsilon(1S)$ our measurements of the branching ratio, the shape of the invariant $\pi\pi$ mass spectrum, the angular distribution of the $\pi\pi$ system, and its decay distribution are consistent with those we obtain for the charged decay $\Upsilon(2S) \rightarrow \pi^+\pi^- \Upsilon(1S)$. In addition we find agreement between our results and those of other experiments.

The ratio of the branching ratios of the neutral pion decay mode to the charged mode indicates consistency with isospin conservation for this decay. The measured angular distributions are consistent with those expected for a spin zero di-pion system emitted in an S-wave. Partial conservation of

axial-vector current (PCAC) together with the observed isotropic angular distributions predicts⁹ the invariant $\pi\pi$ mass spectrum to be peaked at high values as we observe.

ACKNOWLEDGEMENTS

We would like to thank the DESY and SLAC directorates for their support. This experiment would not have been possible without the dedication of the DORIS machine group as well as the experimental support groups at DESY. Some of us (A.F., Z.J., B.N. and G.N.) would like to thank DESY for financial support. A.F. acknowledges financial support by the Deutsche Forschungsgemeinschaft and the Hamburg University. D.W. acknowledges support from a National Science Foundation graduate fellowship. E.D.B., R.H. and K.S. have benefitted from Senior Scientists Awards from the Humboldt Foundation. The Nijmegen group acknowledges the support of FOM-ZWO. The Erlangen, Hamburg, and Würzburg groups acknowledge financial support from the Bundesministerium für Forschung und Technologie and the Deutsche Forschungsgemeinschaft (Hamburg). This work was supported in part by the U.S. Department of Energy under Contract No. DE-AC03-81ER40050 (CIT), No. DE-AC02-76ER03066 (CMU), No. DE-AC02-76ER03064 (Harvard), No. DE-AC02-76ER03072 (Princeton), No. DE-AS03-76SF00326 (Stanford), No. DE-AC03-76SF00515 (SLAC), and by the National Science Foundation under Grants No. PHY81-07396 (HEPL), No. PHY82-08761 (Princeton), No. PHY75-22980 (CIT).

References:

- (†) Present Address: *Institute for Particle Physics, University of California, Santa Cruz, California 95064, USA*
 - (‡) Permanent Address: *DPHPE, Centre d'Etudes Nucléaires de Saclay, Gif-sur-Yvette, France*
 - (§) Permanent Address: *Cracow Institute of Nuclear Physics, Cracow, Poland*
1. B. Niczyporuk *et al.*, Phys. Lett. 100B (1981) 95.
 2. G. Mageras *et al.*, Phys. Rev. Lett. 46 (1981) 1115.
 3. J. Mueller *et al.*, Phys. Rev. Lett. 46 (1981) 1181.
 4. H. Albrecht *et al.*, Phys. Lett. 134B (1984) 137.
 5. D. Besson *et al.*, Phys. Rev. D30 (1984) 1433.
 6. V. Fonseca *et al.*, Nucl. Phys. B242 (1984) 31.
 7. K. Gottfried, Phys. Rev. Lett. 40 (1978) 598.
 8. T.M. Yan, Phys. Rev. D22 (1980) 1652.
Y.P. Kuang and T.M. Yan, Phys. Rev. D24 (1981) 2874.
 9. L.S. Brown and R.N. Cahn, Phys. Rev. Lett. 35 (1975) 1.
 10. G. Abrams, Properties of the New Particles $\psi(3095)$ and $\psi'(3684)$, Proc. of the 1975 Int. Symp. on Lepton and Photon Interaction at High Energies, Ed. W.T. Kirk, (Stanford University, Stanford, 1975).
 11. M. Oreglia *et al.*, Phys. Rev. Lett. 45 (1980) 959.
 12. J. Green *et al.*, Phys. Rev. Lett. 49 (1982) 617.
 13. G. Mageras *et al.*, Phys. Lett. 118B (1982) 453.
 14. The kinematic limit of the acollinearity of leptons originating from $\Upsilon(2S) \rightarrow \pi^0 \pi^0 \Upsilon(1S) \rightarrow \gamma \gamma \gamma l^+ l^-$ is 6° . The larger acollinearity value

used in this analysis also takes into account the uncertainty in the angular measurements of the leptons due to the detector angular resolution and the 2.5 cm DORIS bunch length.

15. We choose not to use the measured electron energies as constraints in the fitting procedure for $\pi^0\pi^0e^+e^-$ events. Using the electron energies does not remove substantial additional background but does reduce the event selection efficiency because of the non-Gaussian tails on the measurements of electromagnetic energies in the Crystal Ball detector. Including the electron energies in the fit biases the confidence level to low values and reduces the selection efficiency.
16. The energy corrections we employ only affect our measurements of the $\pi\pi$ mass distribution (which we present here shortly). We estimate the systematic error due to these corrections by comparing different methods of correction and find the effects to be small compared to the statistical errors on the measurement. The value of the mass difference $M(\Upsilon(2S)) - M(\Upsilon(1S))$ is (563.3 ± 0.4) MeV. Particle Data Group, Rev. Mod. Phys. 56 (1984) No. 2, Part II.
17. R.L. Ford and W.R. Nelson, Stanford Linear Accelerator Center report, SLAC-0210 (1978).
18. M. Voloshin and V. Zakharov, Phys. Rev. Lett. 45 (1980) 688.
19. V.A. Novikov and M.A. Shifman, Z. Phys. C8 (1981) 43.
20. R. Cahn, Phys. Rev. D12 (1975) 3559.

In addition we note that in several previous analyses the pion angular distribution in the di-pion rest frame has been studied in the helicity frame. If the di-pion system is emitted in an S-wave, it can be shown that $\frac{dN}{d\cos\theta_\pi^{hel}} = const$, regardless of the spin of the $\pi\pi$ system. Thus the distribution of $\cos\theta_\pi^{hel}$ cannot analyze the spin of the di-pion system if the latter results from an S-wave decay of the $\Upsilon(2S)$.

21. The average value of $B_{\ell\ell}(\Upsilon(1S))$ is calculated assuming lepton universality and excluding values derived from measurements of hadronic cascade transitions. The value of $B_{\ell\ell}(\Upsilon(1S))$ for each measurement is listed after each reference. Ch. Berger *et al.*, Z. Phys. **C1** (1979) 343 ($2.2 \pm 2.0\%$); Ch. Berger *et al.*, Phys. Lett. **93B** (1980) 497 ($5.1 \pm 3.0\%$); H. Albrecht *et al.*, Phys. Lett. **93B** (1980) 500 ($2.9 \pm 1.3 \pm 0.5\%$); B. Niczyporuk *et al.*, Phys. Rev. Lett. **46** (1981) 92 ($3.5 \pm 1.4 \pm 0.4\%$); D. Andrews *et al.*, Phys. Rev. Lett. **50** (1983) 807 ($2.7 \pm 0.3 \pm 0.3\%$); R. Giles *et al.*, Phys. Rev. Lett. **50** (1983) 877 ($3.4 \pm 0.4 \pm 0.4\%$); The CUSB measurement is taken from: P.M. Tuts, Experimental Results in Heavy Quarkonia, Proc. of the 1983 Int. Symp. on Lepton and Photon Interaction at High Energies, Eds. D.G. Cassel and D.L. Kreinick, (Cornell, Ithaca, 1983) ($2.7 \pm 0.3 \pm 0.3\%$).
22. To calculate the average value of $B(\Upsilon(2S) \rightarrow \pi^+\pi^-\Upsilon(1S))$ we have used the exclusive measurements by LENA ($0.61 \pm 0.21\%$)¹, CUSB ($0.63 \pm 0.13 \pm 0.10\%$)², ($0.56 \pm 0.04 \pm 0.05\%$ for $\pi^+\pi^-e^+e^-$ and $0.52 \pm 0.04 \pm 0.04\%$ for $\pi^+\pi^-\mu^+\mu^-$)⁶, CLEO ($0.74 \pm 0.18\%$)³, ($0.53 \pm 0.05\%$ for $\pi^+\pi^-e^+e^-$ and $0.55 \pm 0.05\%$ for $\pi^+\pi^-\mu^+\mu^-$)⁵, and ARGUS ($0.50 \pm 0.06\%$)⁴ and $B_{\ell\ell}(\Upsilon(1S)) = (2.9 \pm 0.3)\%$. The LENA and ARGUS results are derived from numbers quoted in their publications. The results of the inclusive measurements are taken from ARGUS ($17.9 \pm 0.9 \pm 2.1\%$)⁴ and CLEO ($19.1 \pm 3.1 \pm 2.9\%$)³, ($19.1 \pm 1.2 \pm 0.6\%$)⁵.
23. The form given is derived from a formula in Ref. 8 and explicitly quoted in Ref. 5, 6.

Table 1. The results of the fit of the $M_{\pi\pi}$ mass distributions to different theoretical expressions.

Model	Mass Distribution $\frac{dN}{dM_{\pi\pi}}$	$\pi^0\pi^0$ Result	$\pi^+\pi^-$ Result
Yan ^a	$\propto K \{ (M_{\pi\pi}^2 - 2M_\pi^2)^2 + (\frac{B}{3A})(M_{\pi\pi}^2 - 2M_\pi^2) [(M_{\pi\pi}^2 - 4M_\pi^2) + 2(M_{\pi\pi}^2 + 2M_\pi^2) \frac{K_0^2}{M_{\pi\pi}^2}] + O(\frac{B^2}{A^2}) \}$ $[K_0 = (M_{T'}^2 + M_{\pi\pi}^2 - M_T^2)/(2M_{T'})]$	$\frac{B}{A} = -0.18^{+0.18}_{-0.13}$	$\frac{B}{A} = +0.01^{+0.13}_{-0.11}$
Voloshin-Zakharov ^b	$\propto K(M_{\pi\pi}^2 - \lambda M_\pi^2)^2$	$\lambda = 3.3^{+1.0}_{-1.4}$	$\lambda = 2.1^{+0.7}_{-0.9}$
Novikov-Shifman ^c	$\propto K [M_{\pi\pi}^2 - \kappa(M_{T'} - M_T)^2 (1 + 2\frac{M_T^2}{M_{\pi\pi}^2})]^2 + O(\kappa^2)$	$\kappa = 0.14^{+0.05}_{-0.06}$	$\kappa = 0.08^{+0.03}_{-0.04}$

^a References 8 and 23

^b Reference 18

^c Reference 19

where $K = [((M_{T'} + M_T)^2 - M_{\pi\pi}^2)((M_{T'} - M_T)^2 - M_{\pi\pi}^2)(M_{\pi\pi}^2 - 4M_\pi^2)]^{\frac{1}{2}}$ is the phase space factor.

Figure Captions:

Fig. 1. Scatter plot of the observed $m_{\gamma\gamma}$ masses of the $\gamma\gamma\gamma\gamma\mu^+\mu^-$ and $\gamma\gamma\gamma\gamma e^+e^-$ samples (three entries per event). The box indicates the boundaries of the cut.

Fig. 2. The mass difference $\Delta M = M(\Upsilon(2S)) - M_{recoil}$ where M_{recoil} is the mass recoiling against the 4γ system. The solid curve is the Monte Carlo expectation from energy and angular resolution. The sideband regions are indicated.

Fig. 3. The summed efficiency of the $\pi^0\pi^0 e^+e^-$ and $\pi^0\pi^0\mu^+\mu^-$ decay modes as a function of the invariant di-pion mass.

Fig. 4. The invariant $\pi^0\pi^0$ mass distribution. The histogram is the data without acceptance correction. The solid curve represents the fits to the data of the theoretical expressions folded with the experimental resolution in $M_{\pi^0\pi^0}$ of 8 MeV and the acceptance curve of Fig. 3. The confidence level of all fits is greater than 79%. The dashed curve shows the phase space distribution folded with the acceptance. The agreement between the data and the expectation from phase space has a confidence level of less than 10^{-5} .

Fig. 5. Angular distributions of the $\pi^0\pi^0$ system. The histograms are the data without acceptance correction. The curves represent isotropic distributions corrected for acceptance and normalized to the number of events. a) $\cos\theta_{\pi^0\pi^0}$ distribution. b) $\cos\theta_{\pi^*}^*$ distribution. For a description of the angles see the text. The confidence levels of the agreement between the data and the curves are 3% and 89%, respectively.

Fig. 6. The invariant $\pi^+\pi^-$ mass distribution. The histogram is the data without acceptance correction. The solid curve represents the fits to the data of the theoretical expressions folded with the experimental resolution in $M_{\pi^+\pi^-}$ of 15 MeV and the nearly flat acceptance. The confidence level of all fits is 3%. We have found no systematic effect which can account for this low confidence level and believe it is due to a statistical fluctuation in the highest mass bin.

Fig. 7. Angular distributions of the $\pi^+\pi^-$ system. The histograms are the data without acceptance correction. The curves represent isotropic distributions corrected for acceptance and normalized to the number of events. a) $\cos\theta_{\pi^+\pi^-}$ distribution. b) $\cos\theta_{\pi^\pm}^*$ distribution. For a description of the angles see the text. Note that we do not distinguish between positive and

negative pions. The confidence levels of the agreement between the data and the curves are 43% and 89%, respectively.

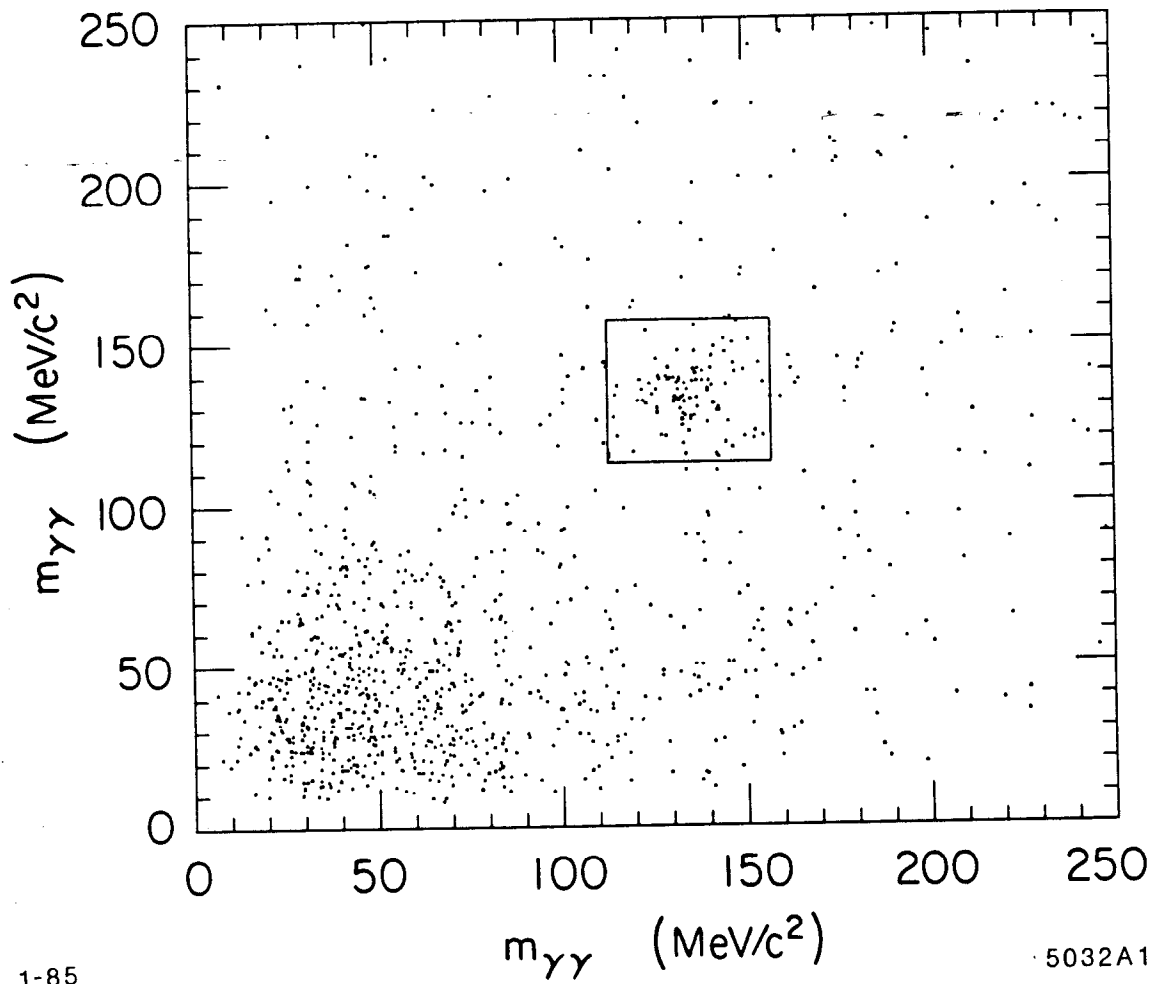


Fig. 1

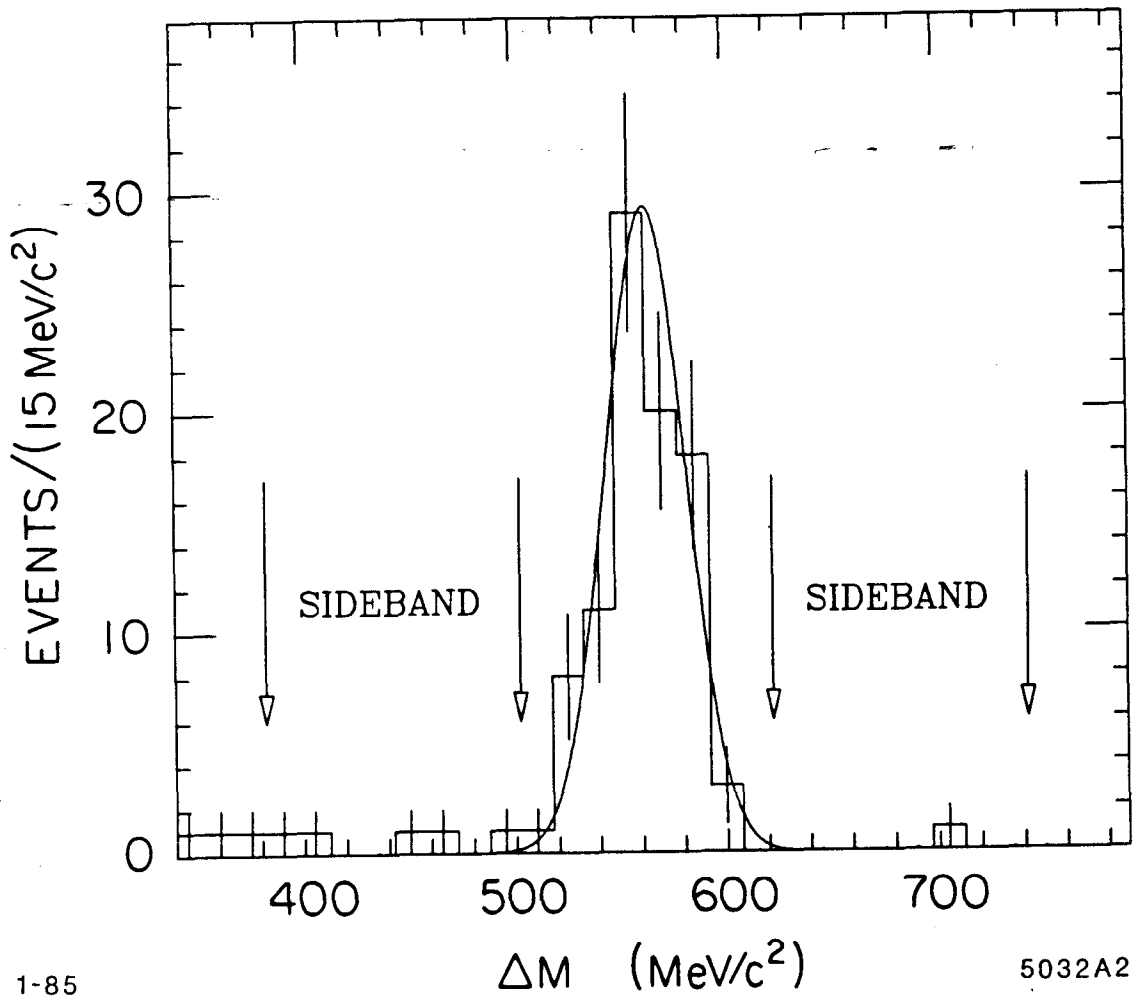


Fig. 2

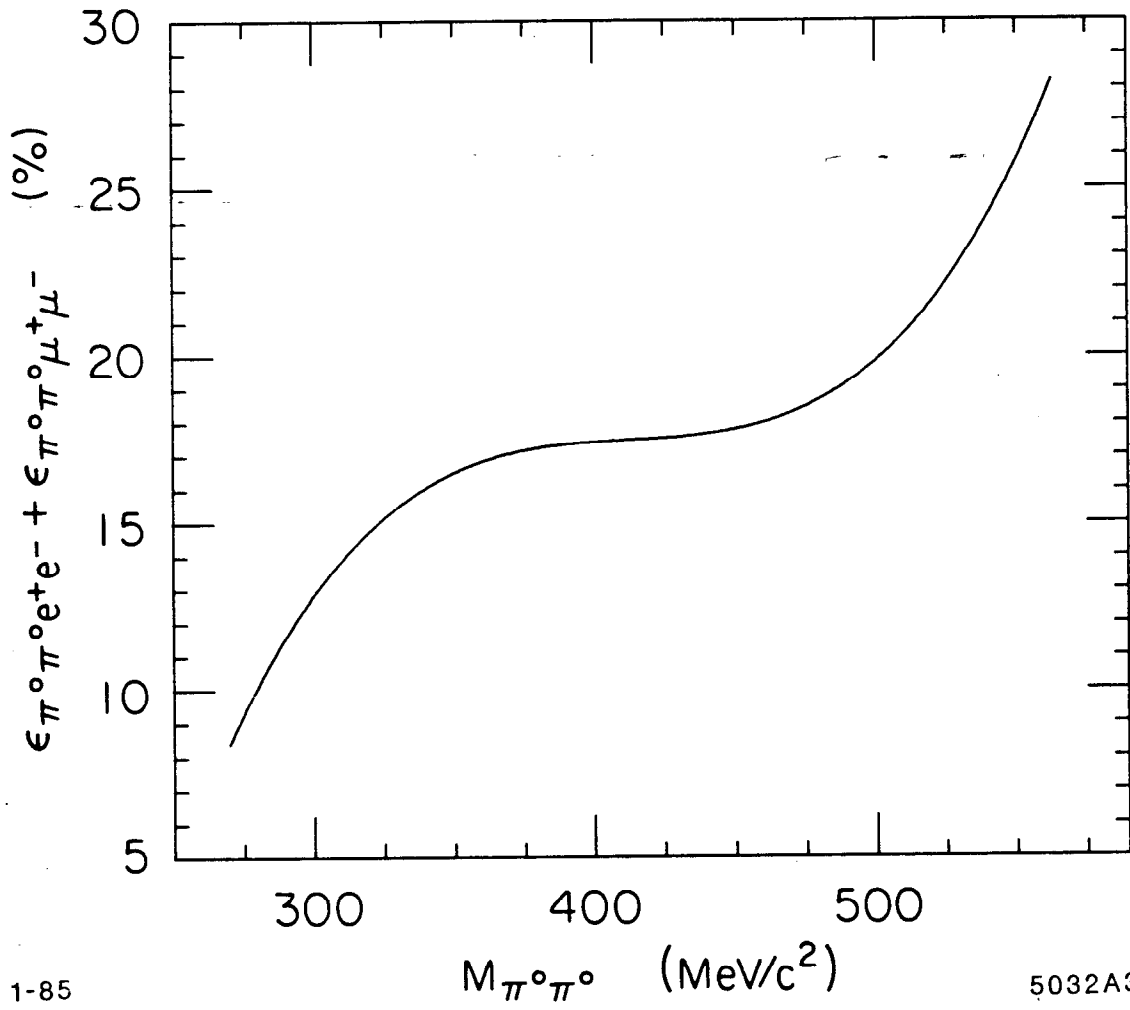


Fig. 3

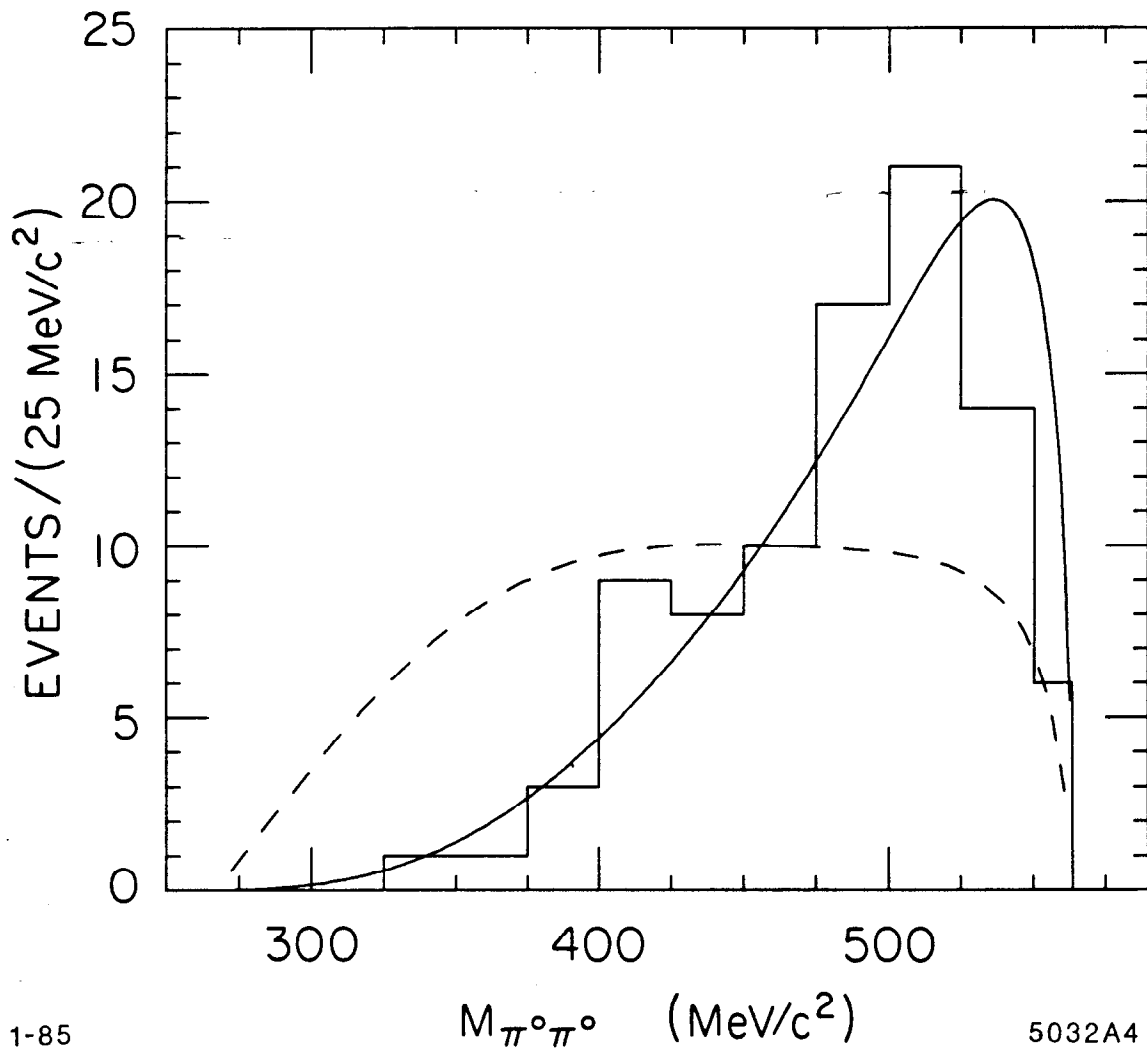
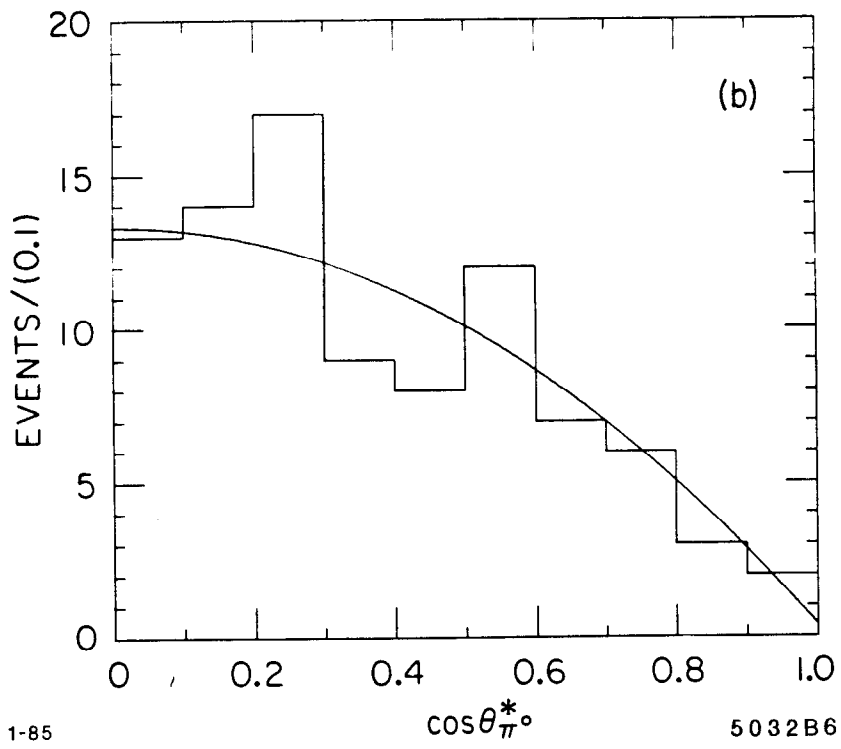
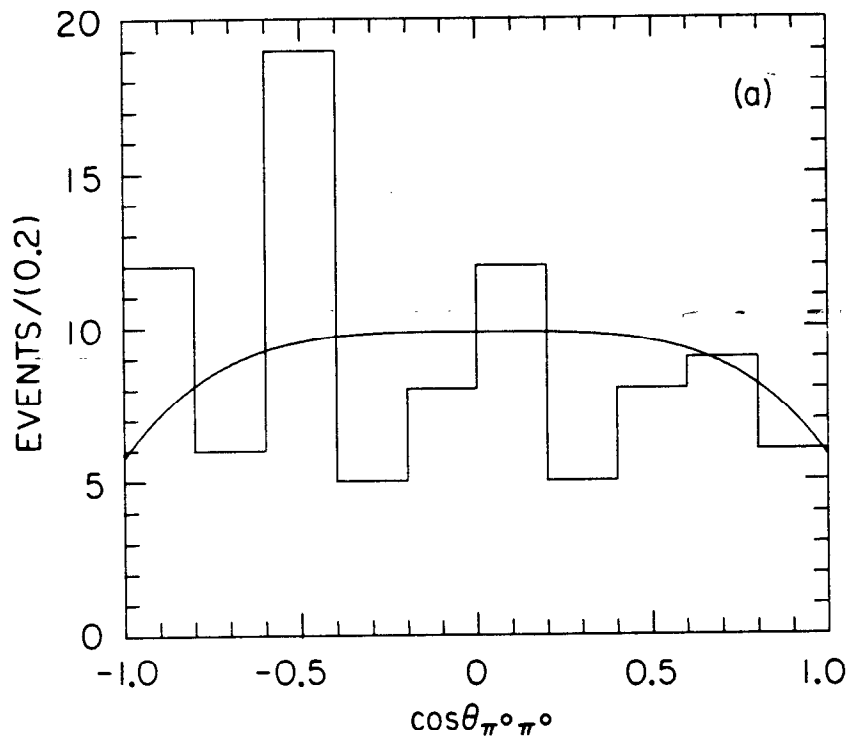


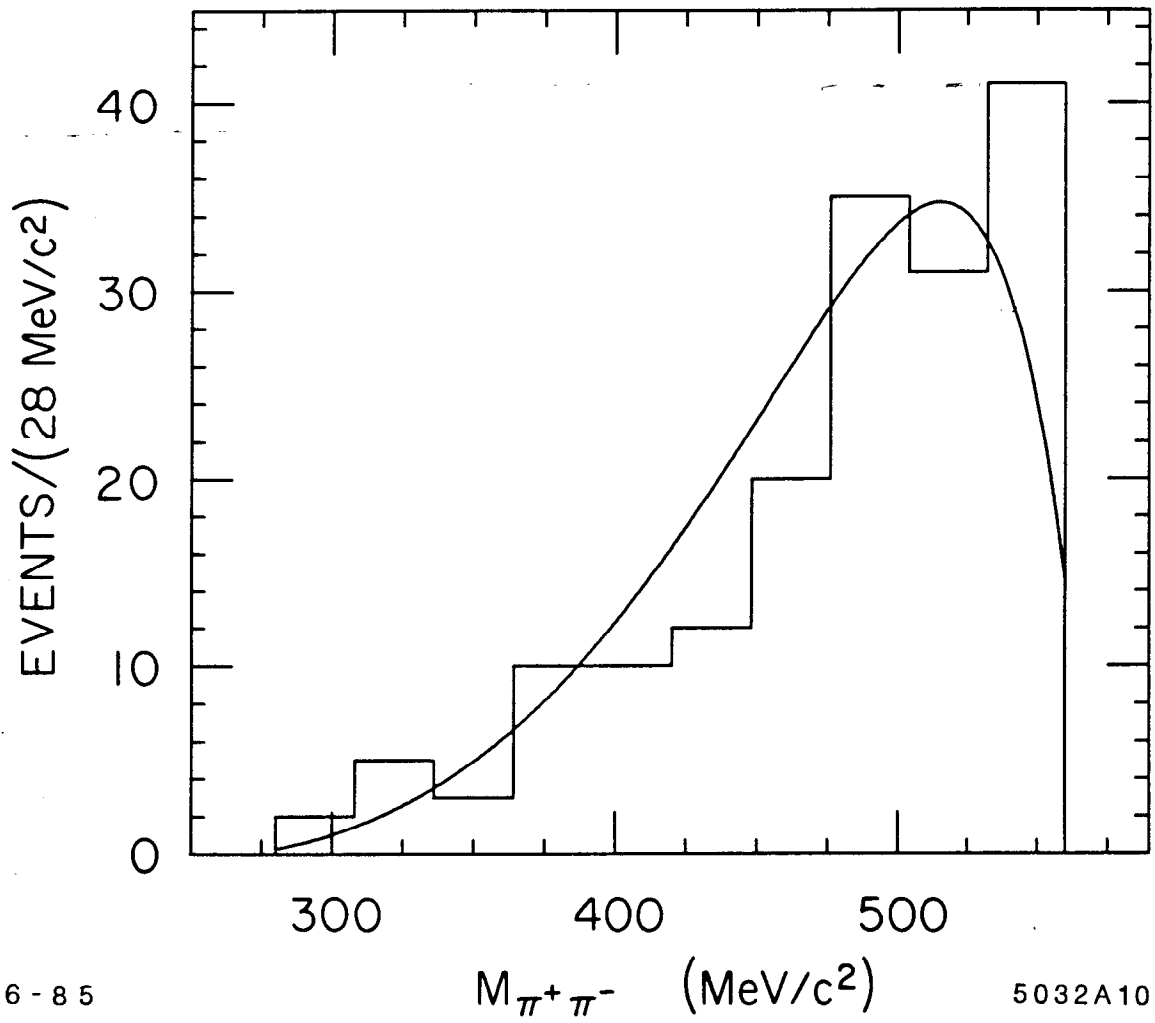
Fig. 4



1-85

5032B6

Fig. 5

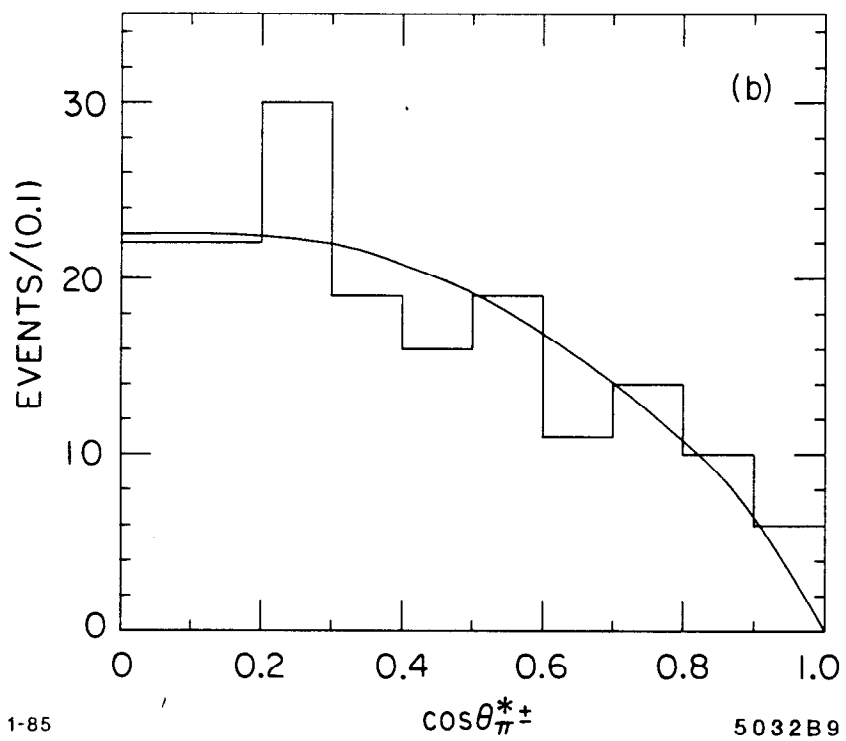
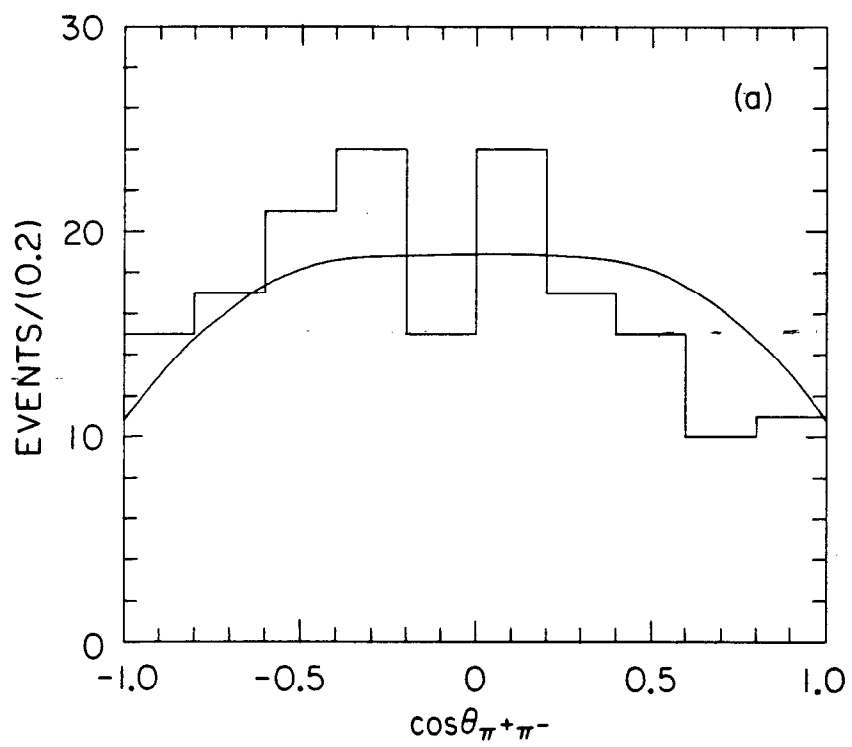


6-85

$M_{\pi^+\pi^-}$ (MeV/c²)

5032A10

Fig. 6



1-85

5032B9

Fig. 7